

Effects of Local Liquid Structure on Orientational Relaxation: 2-Ethyl-naphthalene, Neat and in Solution

S. R. Greenfield,[†] Abhijit Sengupta, John J. Stankus,[‡] M. Terazima,[§] and M. D. Fayer^{*}

Department of Chemistry, Stanford University, Stanford, California 94305

Received: June 7, 1993; In Final Form: October 4, 1993[⊙]

The rotational dynamics of 2-ethylnaphthalene have been studied using subpicosecond transient grating optical Kerr effect techniques. Both the neat liquid and a series of dilutions in carbon tetrachloride were examined. The neat liquid was studied over a temperature range of 2–100 °C, and the 1 M solution was studied from –30 to +25 °C. After ultrafast librational dynamics have decayed, there remains (>2 ps) in the neat liquid a triple-exponential decay of the orientational anisotropy. The slower two decays exhibit hydrodynamic temperature dependences, corresponding to rotational diffusion. The fastest decay is not hydrodynamic, being temperature independent from 2 to 40 °C. This decay is attributed to the relaxation dynamics of local structures in the liquid and is not present in all but the highest concentration (5 M) solution.

Introduction

In this paper we describe the reorientational dynamics of 2-ethylnaphthalene (2EN), studied in the time domain with the transient grating optical Kerr effect (TG-OKE). The orientational dynamics of molecules in liquids have been under intense investigation in recent years using fluorescence depolarization, depolarized light scattering, optical Kerr effect, nuclear magnetic resonance, electron spin resonance, and Raman scattering. OKE experiments are ideally suited for the investigation of very fast (picosecond) and ultrafast (femtosecond) time scale dynamics in systems that exhibit complex time dependencies. Most of the OKE experiments have been done on small or intermediate size molecules such as CS₂,^{1–6} halogenated benzenes,^{7–9} and pyridine.¹⁰ The main goal of these experiments was to investigate ultrafast librational dynamics. The orientational relaxation of these molecules (greater than a few picoseconds) has usually been described by a single exponential, with the exception of iodobenzene⁸ and biphenyl,¹¹ which exhibit biexponential decays.

A recent TG-OKE study of the dynamics of the liquid crystal pentylcyanobiphenyl (5CB) revealed nonhydrodynamic behavior on the 1 ps to 1 ns time scale.¹² The study examined the orientational relaxation of 5CB in its isotropic phase near the nematic phase transition. Within a range of temperatures above the nematic/isotropic phase transition, the macroscopically isotropic liquid has a high degree of local structure, forming microscopic pseudonematic domains.¹³ The orientational relaxation from a few picoseconds to a nanosecond exhibits a complex time dependence that is temperature independent over a temperature range in which the viscosity of the liquid changes by a factor of 3. This totally nonhydrodynamic behavior was discussed in terms of relaxation on a free energy potential surface fixed on the time scale of the relaxation and not in terms of rotational diffusion. The OKE perturbs local structures that are at minima of their free energy surfaces. The time dependence on the picosecond to nanosecond time scale involves relaxation back to local minima, not orientational randomization of the local structures. The long time scale (tens to hundreds of nanoseconds) orientational relaxation of 5CB is described very accurately by the Landau–de Gennes theory which predicts a temperature dependence that is proportional to the viscosity, $\eta(T)$, and inversely

proportional to $T-T^*$, where T^* is the isotropic/nematic phase-transition temperature.¹³ The long time behavior (the randomization of the pseudonematic domains) is analogous to hydrodynamic behavior of a simple liquid. Virtually identical behavior has recently been observed in another liquid crystal system, methoxybenzylidenebutylaniline (MBBA)¹⁴ which has a different molecular structure.^{12,14}

Another example of the influence of local structure on molecular motions can be found in polymer solutions. The dynamics of poly(2-vinylnaphthalene) (P2VN) in CCl₄ have been explored using the TG-OKE.^{15a} The experiment measured motions of the naphthyl side groups. In addition to the librational decay, there are two slower orientational relaxation components present. Temperature changes did not affect either of these decay rates, although η/T changed by a factor of 30. Very recently, the side group dynamics of poly(methylphenylsiloxane) were observed to be viscosity/temperature independent although η/T changed by a factor of 40.^{15b} The η/T independent dynamics of these polymer side groups are described in terms of the local structure determined by the backbone and the steric interactions of the side groups.¹⁵

In the experiments presented below, neat 2EN exhibits a behavior that is analogous to that observed in the liquid crystals and polymer systems although it is a normal molecular liquid. The slowest dynamics are composed of a biexponential decay that displays hydrodynamic behavior. However, there is an additional fast relaxation process that displays no temperature dependence over a significant range of temperatures. This nonhydrodynamic behavior is described in terms of relaxation of local structures in the liquid rather than orientational diffusion. Dilution of 2EN in carbon tetrachloride eliminates the local structures in the liquid, and a hydrodynamic biexponential decay is observed at all but the highest (5 M) concentration.

Experimental Procedures

The experiments described here were performed using a subpicosecond laser system that has been described in detail elsewhere.¹⁶ The DCM dye laser was tuned to 665 nm and provided 300 fs, 10 μ J pulses at a repetition rate of 1.75 kHz. The wavelength was chosen to prevent two-photon absorption.

In the TG-OKE experiment,¹¹ typical excitation and probe pulse energies were 0.5 and 0.2 μ J, respectively. The excitation beams are orthogonally polarized, forming a polarization grating.¹⁷ This configuration results in an excellent signal/noise ratio. It also prevents the formation of acoustic waves, which would interfere with the signal at long times.¹⁸ A polarizer is put in the signal path, eliminating (nondepolarized) scattered light from

[†] Current address: Chemistry Division, Argonne National Laboratory, Argonne, IL 60439.

[‡] Current address: IBM Almaden Research Center, San Jose, CA 95120.

[§] Current address: Department of Chemistry, Faculty of Science, Kyoto University, Kyoto 606, Japan.

^{*} Abstract published in *Advance ACS Abstracts*, December 1, 1993.

the nearby excitation beam. A different polarization configuration allowing for separation of the electronic and nuclear responses of the OKE is used for acquiring the librational decays (*vide infra*).

The signal is detected by a photomultiplier tube (PMT). The output of the PMT is measured with a gated integrator, using the single-shot (nonaveraging) mode. A second gated integrator is used to measure the intensity of each laser shot. The outputs of the gated integrators are digitized by computer. The computer monitors the intensity of each pulse, and the signal is averaged in when the intensity falls within a preset window. Typically, a window of $\pm 10\%$ was used. On every other shot, the probe beam was blocked by a mechanical chopper. A normalized background was subtracted from the "signal shot", thus mimicking the background signal rejection capabilities of a lock-in amplifier. Data sets were typically the average of 30 delay line scans, with each scan taking approximately 1 min.

The 2EN came from Aldrich, and spectroscopic grade CCl_4 was used for the dilution studies. Both chemicals were used without further purification. The samples were filtered through a Gelman 0.2- μm Acrodisc CR filter to remove dust. The 2EN sample was placed in a 1-mm spectrophotometric cuvette. For temperatures above room temperature, the cell was mounted inside an aluminum block heated by resistive heating wire. The temperature was regulated and held constant to $\pm 0.1^\circ\text{C}$ by a proportional temperature controller. Below room temperature, the cell was mounted in a thermoelectrically cooled metal block that could be held constant to $\pm 0.3^\circ\text{C}$.

Sample viscosities were measured over the investigated temperature range with a Cannon-Ubbelohde viscometer (IGR). Two different viscometers were used, one covering the kinematic viscosity range of 0.5–2 centistokes, and the other 2–8 centistokes. Shear viscosity was calculated by multiplying the kinematic viscosity by the sample density. Densities as a function of temperature were calculated with the isobaric expansion formula using the coefficient of benzene.

Results and Discussion

The problem of an anisotropic rotational diffuser was solved by Favro.¹⁹ The result of the application of the solution to the molecular polarizability correlation function (the fundamental correlation function for DLS and OKE experiments) yields a correlation function given, in general, by the sum of five exponentials²⁰

$$C_{\text{VH}}^{\alpha}(t) \propto \sum_{n=1}^5 A_n e^{-f_n t} \quad (1)$$

where the coefficients A_n and the exponential terms f_n are given in ref 20, and the subscript VH refers to depolarized light scattering (the equivalent to the polarization grating OKE experiment). This correlation function was shown to be related to the dielectric impulse response function (the square of which is the TG-OKE observable) by time differentiation²¹

$$G_{\text{ijj}}^{\alpha}(t) = -16\pi^2 \frac{\theta(t)}{k_B T} \frac{\partial}{\partial t} C_{\text{VH}}^{\alpha}(t) \quad (2)$$

where $\theta(t)$ is the unit step function. Combining these two equations gives us

$$G_{\text{ijj}}^{\alpha}(t) \propto \sum_{n=1}^5 A_n f_n e^{-f_n t} \quad (3)$$

Equations 1 and 3 give the observables for DLS and OKE experiments, respectively. Although they are almost identical, the difference between them is part of the reason why the OKE has advantages compared to DLS for measuring fast and ultrafast orientational dynamics. The presence of the f_n term in the

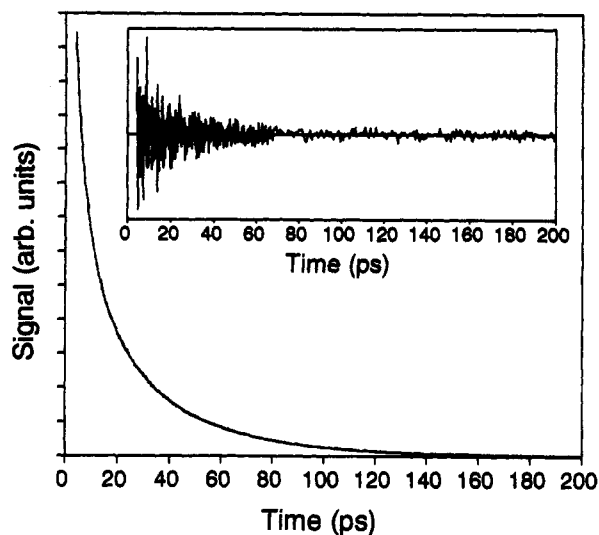


Figure 1. Transient grating optical Kerr effect signal for neat 2-ethyl-naphthalene following the ultrafast librational dynamics at 25°C . The fit to the triple-exponential model is also shown. The greatly magnified residuals of the fit are shown in the inset.

amplitude of the OKE observable means that the amplitude of the contribution is proportional to the rate of orientational relaxation. Thus, faster decays have inherently greater amplitude than slower decays and are thus easier to observe. For a molecule in which the moment of inertia tensor and the polarizability tensor coincide, or nearly coincide, a biexponential will be observed following the ultrafast librational dynamics. This is observed for 2EN in dilute solution.

Following the librational dynamics, however, the neat 2EN data presented below can be accurately decomposed into the sum of three exponentials,

$$G_{\text{ijj}}^{\alpha}(t) = \sum_{m=1}^3 a_m e^{-t/\tau_m} \quad (4)$$

Comparison of these last two equations gives $a_m = f_n A_n$ and $\tau_m = 1/f_n$. We will show that actually only two of the three experimentally measured decays correspond to (rigid rotor) rotational diffusion.

Figure 1 shows data and fit for neat 2EN out to 200 ps at 25°C . Because the signal from a TG-OKE experiment is proportional to the square of the impulse response function, we use the square of eq 4 in our analysis to fit the raw data. The data are well fit by a triple exponential, as can be seen by the residuals shown in the inset. This decay, as with all of the postlibrational data, is scanned out until the signal reaches the baseline using a polarization grating. Because the data in these scans are not analyzed until several picoseconds after $t = 0$ (many times the optical pulse length), the electronic OKE response does not affect the data, and the use of a polarization grating is justified. Similarly, the finite instrument response does not affect the data at these times, so convolutions are unnecessary.

Any attempt to fit the data with less than three exponentials was unsuccessful, producing poor residuals. Since any decaying function can be fit to the sum of enough exponentials, it is essential to establish that the data are truly the sum of three "legitimate" exponentials. Figure 2 shows semilog plots (all logarithmic plots employ the natural logarithm) of the polarization grating data. The logarithm of the slowest component is shown in Figure 2a. The data are clearly single exponential for 7 factors of e , with a time constant given by τ_s ($s \equiv$ slow). As the measured signal is proportional to the square of the sample response function, the square roots of the data are taken to eliminate cross terms before the slow decay can be subtracted off. A semilog plot showing the square root of the data with the slow component properly

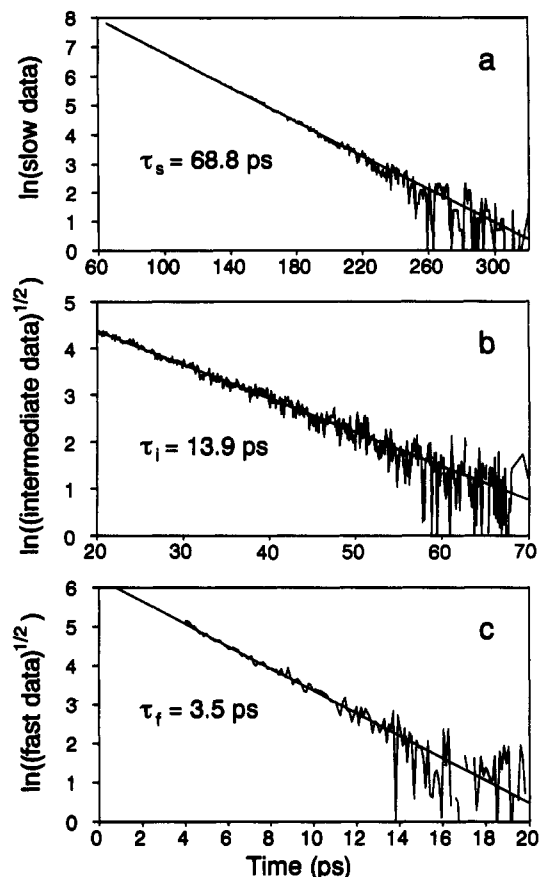


Figure 2. Semilog plots of the neat 2EN data at 25 °C with single-exponential fits to each of the three components. The y-axis scales factors of e. (a) Slow component: logarithm of the raw data showing the single-exponential tail of the decay over 7 factors of e. (b) Intermediate component: logarithm of the square root of the data minus the fit to the slow component. This component spans 7 factors of e of the signal. (c) Fast component: logarithm of the square root of the data minus the fit to the slow and intermediate components. This component spans 8 factors of e of the signal.

subtracted off is shown in Figure 2b. It is single exponential for 7 factors of e of the signal (3.5 factors of e of the square root of the signal), with a time constant given by τ_i (i = intermediate). Figure 2c shows the logarithm of the square root of the data with both the slow and intermediate components properly subtracted off. It is single exponential for 8 factors of e of the signal (4 factors of e of the square root of the signal), with a time constant given by τ_f (f = fast). The decay constants are $\tau_s = 68.8$ ps, $\tau_i = 13.9$ ps, and $\tau_f = 3.5$ ps. The substantial amplitudes and clear separation of time scales of the three decays provide a high level of confidence in the use of the triple-exponential function to describe the postlibrational data in neat 2EN.

Molecular motions that occur on a picosecond or longer time scale can generally be adequately described by a modified Debye–Stokes–Einstein (DSE) theory. The original DSE theory solves the problem of a rotating sphere in a featureless continuum. The rotational diffusion time constant τ is given by

$$\tau = \frac{V\eta}{k_B T} \quad (5)$$

where V is the volume of the rotating particle, η is the shear viscosity of the fluid, T is the temperature, and k_B is the Boltzmann constant.^{22,23} This theory assumes stick boundary conditions; i.e., the first layer of fluid surrounding the rotating particle sticks to the particle. Extension of the theory to include the behavior of more complex shapes (ellipsoids) was done by Perrin.²⁴

The modified DSE theory with stick boundary conditions works well to describe the rotation of large particles. It significantly

overestimates the rotational times for molecules, however. This implies that a more appropriate boundary condition for molecular scales is one that involves less rotational “friction”. Under slip boundary conditions, the friction is due only to the displacement of the fluid by the asymmetric particle. Hu and Zwanzig calculated correction factors for the problem of oblate and prolate spheroids with slip boundary conditions.²⁵ Youngren and Acrivos extended the theory to ellipsoids by calculating frictional coefficients λ_i for motions about the three axes of an ellipsoid with slip boundary conditions.²⁶ These frictional coefficients replace both the Perrin shape factor and the Hu and Zwanzig slip boundary condition correction factor.

The application of the modified DSE equation to the experimental analysis of rotational diffusion of molecules in liquids has shown the necessity of the inclusion of an additional term, τ_0 .²⁷ The nonzero intercept was found to be necessary to properly fit the η/T dependence for many molecules. τ_0 is the value of τ for η/T extrapolated to zero. It has been observed that the value of τ_0 necessary to fit the experimental data can be either positive or negative, and there is currently no evidence that τ_0 contains any real molecular information.²³

The development for rotational diffusion and hydrodynamic theory so far is accurate in the case of a dilute solution. One needs to consider the effects of high-concentration solutions or neat liquids. The correlation function measured by the OKE and light scattering is a multiparticle correlation function. This is distinctly different from NMR and fluorescence experiments, for example, which measure single-particle correlation functions. Keyes and Kivelson²⁸ have shown that although the single-particle and two-particle correlation function terms may relax with different correlation times, the total correlation will relax with a single correlation time. Specifically, if the single-particle correlation function relaxes as a single exponential with a time constant τ , then the total correlation function relaxes as a single exponential with a time constant τ_c , related by^{28,29}

$$\tau_c = \frac{g_2}{j_2} \tau \quad (6)$$

where g_2 is the static orientational correlation parameter and j_2 is the dynamic orientational correlation parameter.

In general, it appears that the dynamic correlation parameter j_2 is approximately unity.²³ The static correlation factor can be independently determined by integrated light scattering intensities.²⁰ If the assumption that $j_2 \approx 1$ is made, then g_2 can also be determined by comparison of the results of an experiment that measures τ_c with an experiment that measures τ . This approach was pioneered by Alms *et al.*, using DLS and NMR.³⁰ If one also makes the assumption that the hydrodynamic boundary conditions remain unchanged by dilution, then one can simply determine g_2 by comparison of τ_c for the neat liquid with τ_c for a dilute solution. This is the approach that will be used here. Thus, the DSE equation in its final form is

$$\tau_c = g_2 \left(\frac{\lambda V \eta}{k_B T} \right) + \tau_0 \quad (7)$$

where the Youngren and Acrivos frictional coefficient and the nonzero intercept have also been included. The subscripts for the (up to) five different correlation times have been suppressed for clarity.

A comparison of the data to hydrodynamic (DSE) theory requires that the rotational diffusion time constants be plotted versus the viscosity divided by the absolute temperature, with the viscosity measured over the desired temperature range. The viscosity of neat 2EN is shown as an Arrhenius plot in Figure 3. The data are clearly not fit by a single activation energy (i.e., not a straight line). The fit shown uses two different activation energies. For temperatures below 20 °C, $E_a = 19.1$ kJ/mol, while for temperatures above 20 °C, $E_a = 14.3$ kJ/mol. As can

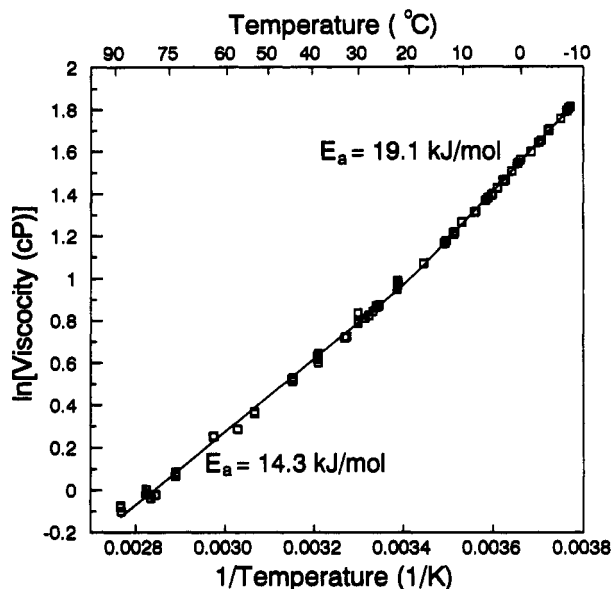


Figure 3. Arrhenius plot of the viscosity of neat 2EN. The viscosity at temperatures below 20 °C is fit with an activation energy of 19.1 kJ/mol. Above 20 °C the activation energy is 14.3 kJ/mol.

be seen, the data are very well fit by the use of a different activation energy at lower temperatures. The 1 M 2EN in CCl_4 solution was well fit by a single activation energy ($E_a = 11.2$ kJ/mol), which is far more characteristic of the behavior of simple liquids.

The temperature dependence of the slow decay of neat 2EN from 2 to 100 °C is shown in Figure 4a. Each temperature point is the average of several data sets. The error bars (\pm the standard deviation of the different data sets at each temperature) are not shown, as they are roughly the size of the symbols. The dynamics clearly are hydrodynamic, following a DSE equation of the form $\tau = C\eta/T + \tau_0$. A linear least-squares fit to the data gives $\tau_s = (8090 \pm 80 \text{ ps K/cP})(\eta/T) + (1.9 \pm 1.9) \text{ ps}$. The temperature dependence of the intermediate decay from 2 to 80 °C is shown in Figure 4b. While the error bars are greater than those for the slowest decay, the rotational diffusion time constant again obeys the DSE equation. The fit for the intermediate data gives $\tau_i = (960 \pm 47 \text{ ps K/cP})(\eta/T) + (4.3 \pm 1.6) \text{ ps}$.

A dilution study of 2EN in CCl_4 was undertaken for a variety of reasons. Most importantly, the dilution study provides a great deal of insight into the nature of the triple-exponential decay in neat 2EN. Also, as discussed above, the observable measured in DLS and OKE experiments is not a single-particle quantity. The exact relation between the observed "collective" time constant and the single-particle time constant was given in eq 6. The single-particle rotational diffusion time constant can be exactly determined using one of these experimental techniques only if the sample is an infinitely dilute solution. In practice, the experiment can be performed at several dilutions. If the time constants cease to change with decreasing concentration (keeping η/T constant), then the single-particle time constant has been measured. This also allows us to determine the static orientational order parameter g_2 .

The choice of the solvent was not an arbitrary one. In addition to the obvious constraint of solubility, the ideal solvent should have a viscosity similar to that of neat 2EN and have little or no OKE response of its own. Initially, a number of alkanes were tried, but they had a weak OKE response that could not be easily separated from the slowest 2EN decay. Neat CCl_4 also has an OKE response. Because of the tetrahedral symmetry of CCl_4 , the signal cannot arise from reorientational dynamics but rather must be due to collision-induced (CI) effects (*vide infra*). The signal is weak compared to the 2EN signal, and commensurate with a CI effect response, the decay is very fast (only slightly longer than the pulse length). To achieve overlap of the solution

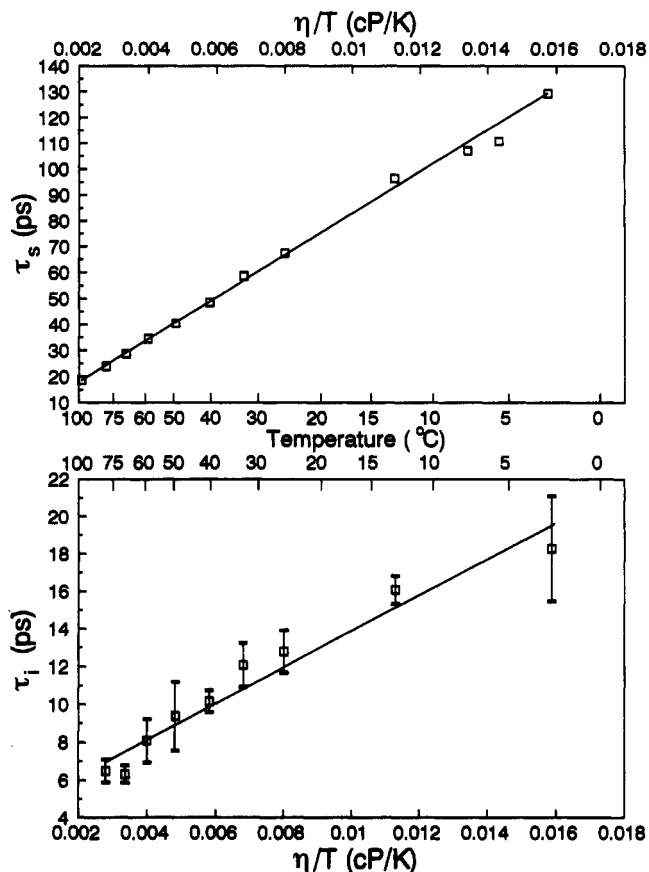


Figure 4. Viscosity/temperature dependences of the rotational diffusion components of the neat 2EN decay. (a) Slow component: τ_s from 2 to 100 °C. The error bars are roughly the size of the symbols. (b) Intermediate component: τ_i from 2 to 80 °C. The error bars show the ± 1 standard deviation spread on τ_i at each temperature. The straight line fits in a and b show hydrodynamic behavior for both decay components. Note the temperature scale between a and b and the viscosity/temperature (η/T) scales at the top and bottom.

viscosities with those of neat 2EN, the solution data were taken at or below room temperature.

Four different concentrations of 2EN in CCl_4 were used in the TG-OKE dilution experiments: 0.5, 1, 3, and 5 M (neat 2EN is 6.35 M). The mole fraction of 2EN in these solutions is 0.050, 0.10, 0.36, and 0.70, respectively. Polarization grating experiments were performed on these solutions at 25 °C. Figure 5 shows data and fit to 100 ps for 1 M 2EN in CCl_4 at 25 °C. Following the ultrafast librational dynamics, the lowest three concentrations are cleanly fit with a biexponential model function, as opposed to the triexponential used to fit the neat 2EN data. In addition, the 1 M solution was examined at 11 temperature points between -30 and +25 °C. The temperature dependence of the solution data is shown in Figure 6. The neat data for τ_s and τ_i are also shown for comparison. Two observations about the 1 M data are immediately obvious. The first is that both components are clearly hydrodynamic, being well fit by straight lines. To avoid confusion with the neat data components, the solution data rotational diffusion time constants will be referred to as τ_{ss} (ss = solution slow) and τ_{sf} (sf = solution fast). No explicit assumptions are being made yet as to the relationship between the neat and solution decay components. A linear least-squares fit to the slower decay for the 1 M 2EN data in Figure 6a gives $\tau_{ss} = (4220 \pm 120 \text{ ps K/cP})(\eta/T) + (5.2 \pm 1.5) \text{ ps}$. The fit to the faster decay shown in Figure 6b gives $\tau_{sf} = (218 \pm 40 \text{ ps K/cP})(\eta/T) + (2.4 \pm 0.5) \text{ ps}$.

The second observation from Figure 6 is that neat data and the solution data do not overlap. There are (at least) two possibilities for this. The first is that the decays shown do not directly correspond to the same physical processes (i.e., the same

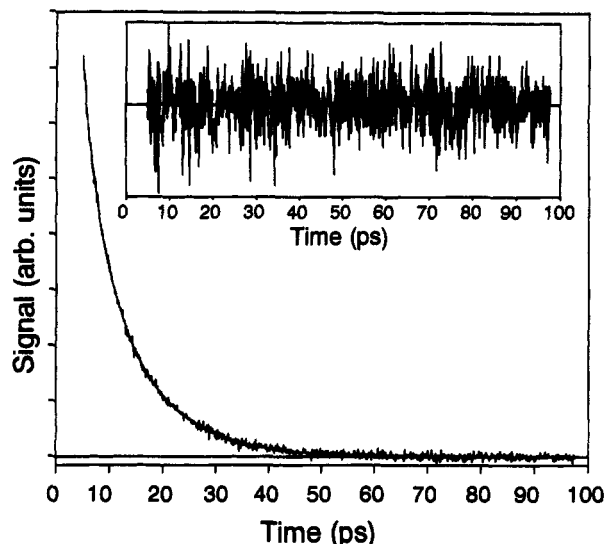


Figure 5. Transient grating optical Kerr effect signal for 1 M 2-ethynaphthalene in CCl_4 at 25 °C. The fit to a biexponential model is also shown. The residuals, greatly magnified, are displayed in the inset.

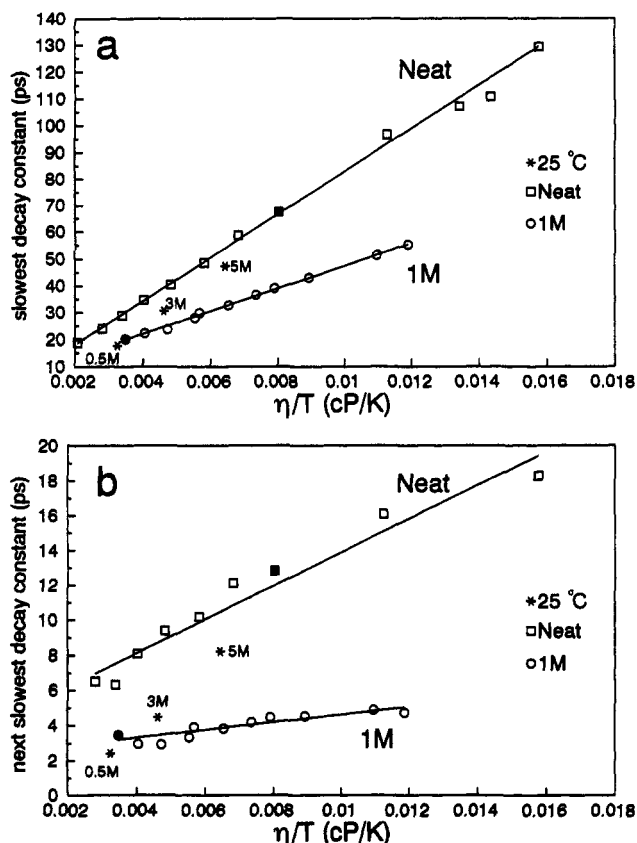


Figure 6. Viscosity/temperature dependences of the rotational diffusion components of the decay for the various 2EN/ CCl_4 solutions. The neat data from Figure 4 are also shown for comparison: (a) slowest component, τ_{ss} ; (b) next slowest component, τ_{sf} . The 1 M 2EN/ CCl_4 temperature range was -30 to $+25$ °C for both a and b. The error bars are not shown for clarity but are somewhat greater than those of the neat data.

rotations). The other possibility is that the decays do indeed correspond, and the difference in the slopes (effective hydrodynamic volumes) is due to the multiparticle contribution to the neat 2EN OKE observable (i.e., $g_2 \neq 1$). While neither of these possibilities can be unequivocally ruled out, we will provide evidence that the second case is the more likely one.

The ability of a biexponential to fit the dilute 2EN solutions is very significant. As discussed above, the solution for the rotational diffusion of an anisotropic rigid rotor is given by the

sum of five exponentials with decay rates f_{1-5} . If the principal axis systems for the moment of inertia tensor and the polarizability tensor coincide, the number of exponentials is reduced to two, with only the f_1 and f_2 terms having nonzero amplitudes. The amplitudes of the three additional decays increase as the difference between the two axis systems increases. In 2EN is fit by a biexponential (the significance of the third exponential in neat 2EN will be discussed later).

The observation of a biexponential decay in the solution 2EN data can be compared with predictions of the amplitudes and time constants of the (at most) five theoretical decays using eq 3. The ethyl group of 2EN can exist in three configurations, with the out-of-plane orientation having by far the least steric hindrance. This configuration was used for both the volume and polarizability calculations. Calculations using a Stuart-Briegleb space filling model of 2EN and the formalism developed by Youngren and Acrivos²⁶ to predict the hydrodynamic volume of 2EN show that the slowest component must be f_2 . The polarizability of 2EN was calculated by adding the polarizability of naphthalene³¹ and the ethyl group, with the ethyl group in the out-of-plane orientation. The polarizability of the ethyl group was estimated by adding the polarizabilities of the C-C and C-H bonds.³² In addition to being the slowest decay, f_2 also has the greatest amplitude, which matches the experimental data for both neat 2EN and the solution data. With the slowest experimentally observed decay corresponding to f_2 , it follows that $\tau_{ss} = 1/f_2$ for the solution data and $\tau_s = 1/f_2$ for the neat data. If 2EN is approximated to be a symmetric diffuser (i.e., rotations about the two short axes are equivalent), then $f_2 = 6\Theta_{\perp}$ and the slowest component corresponds exclusively to the "tumbling" motion of the molecule.

With the assignment of f_2 to the slowest experimental decay, the only remaining theoretically-predicted decay that has any appreciable amplitude is f_1 . For the solution 2EN data, the remaining experimental decay (τ_{sf}) therefore must correspond to f_1 . The assignment of which of the two remaining components for neat 2EN is less unambiguous. The uncertainties in the calculations of the experimental amplitudes and time constants make it difficult to assign f_1 to one of the two possible decays from these calculations alone. The most convincing evidence that $\tau_1 = 1/f_1$ is seen in Figure 6. For both the slowest (a) and next slowest (b) decays, the time constants for the 3 and 5 M 2EN solutions make a smooth transition from the 1 M line to the neat line. The explanation for the transition is the increase of g_2 with concentration. A transition from τ_{sf} to τ_f would not be readily explainable, as τ_f is faster than τ_{sf} for all concentrations.

Now that it has been determined that $\tau_s = \tau_{ss} = 1/f_2$ and $\tau_1 = \tau_{sf} = 1/f_1$, the value for g_2 can be estimated. Looking at the behavior of the 25 °C data in Figure 6 (denoted by an asterisk), it is unclear whether the 1 M data is representative of the true single-particle dynamics. The data are sufficiently noisy to make it difficult to determine if the 0.5 M data actually fit on the 1 M data line, although it certainly appears to be close. Nevertheless, for the neat liquid, we can put a lower bound on the value of g_2 . For the slow decay (tumbling), $g_2 \geq 2$, and for the faster decay (a combination of spinning and tumbling) $g_2 \geq 4$. If we assume that $g_2 \approx 1$ for the 1 M data, then the single-particle "effective" hydrodynamic volume (λV) of the tumbling rotation can be calculated with eq 7 to be $58 \pm 2 \text{ \AA}^3$.

Figure 7 shows the temperature dependence of the fast component of neat 2EN from 2 to 80 °C. The behavior of this component of the orientational anisotropy relaxation is nonhydrodynamic. The value for τ_f is temperature independent from the lowest temperature at which we made measurements (2 °C) to 40 °C. Above 40 °C, τ_f becomes temperature dependent. In the temperature-independent regime, the viscosity of the liquid changes by a factor of 2.1, and τ_s and τ_1 change by factors of ≈ 3

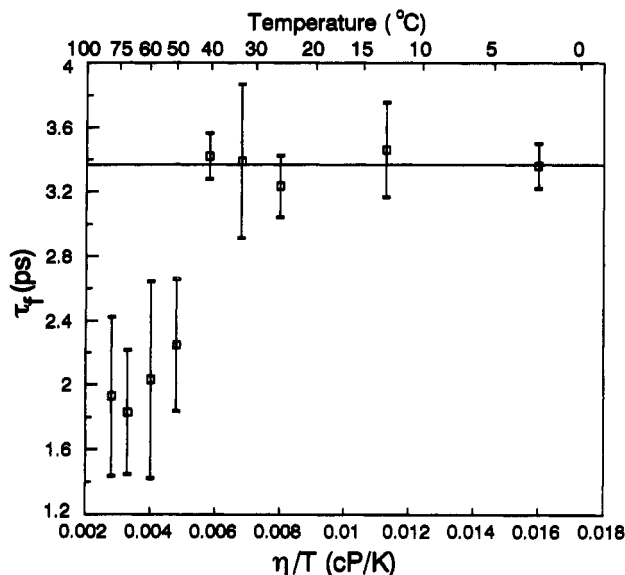


Figure 7. Viscosity/temperature dependence of the fast component (τ_f) of neat 2EN from 2 to 80 °C. The straight line shows the average of the 2–40 °C data ($\tau_f = 3.36$ ps). The data are viscosity/temperature independent from 2 to 40 °C, showing the nonhydrodynamic behavior of the orientational dynamics.

and ≈ 2 , respectively. Thus over a range of temperatures in which any mode of hydrodynamic rotational diffusion should change significantly, τ_f is associated with reorientational relaxation that is clearly nonhydrodynamic.

Because the 1 M 2EN data is well described by a biexponential decay, the additional component, τ_f , seen in the neat data must be associated with a dynamic phenomenon that is not anisotropic rigid rotor rotational diffusion. We propose that τ_f is the time for local structure relaxation, in analogy to the liquid crystal^{12,14} and polymer¹⁵ systems discussed in the Introduction. In liquid naphthalene (as in benzene), pairs of molecules are known to form a somewhat crooked "T" shaped structure.³³ It is reasonable to assume that 2EN forms similar structures. Dilute 2EN in CCl_4 will not have these structures, and τ_f is not observed in the dilution experiments.

On a time scale fast compared to the rotational diffusion times (time scale for randomization of orientations), local structures in the neat liquid are associated with local, momentary minima on a free energy surface. The optical field perturbs the local structure. With the electric field on, the potential surface is changed, and local structure is no longer at the potential minimum. The local structure thus starts evolving toward the new minimum. After the optical pulse is over, the electric field is gone and the local structure has evolved away from the zero-field potential minimum. The local structure will now relax toward the (zero-field) potential minimum. It is this relaxation time that we associate with τ_f . It is not anisotropic rigid rotor rotational diffusion. Evidence for potentially similar low-frequency collective modes in simple liquids has recently been observed in benzene and pyridine.³⁴

The polarizability of 2EN is greatest along the length of the molecule.³¹ Thus, the result of the optical pulse is to slightly align the molecules, primarily along their long axis. Such alignment involves a disturbance of the crooked "T" shape of the neighboring 2EN molecules. After the relaxation back to the "crooked T's", one is left with a collection of partially aligned crooked T's. This leaves a residual anisotropy. It is the randomization of this residual anisotropy that is responsible for the anisotropic rigid rotor rotational diffusion components (τ_i and τ_s) of the decay.

Figure 8 displays the dynamics of the sample anisotropy, S , schematically. At $t = 0$, $S = 0$. The sample is an isotropic liquid with zero macroscopic anisotropy. When the field is applied

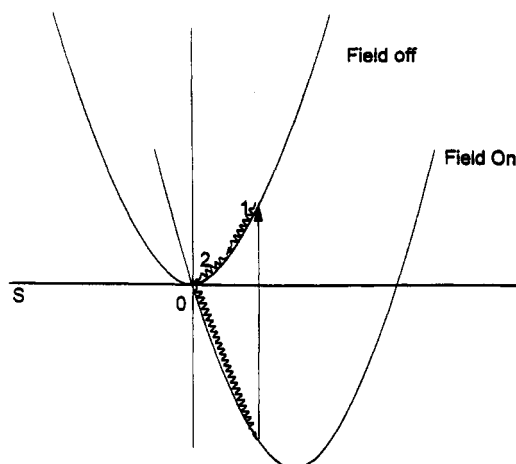


Figure 8. Schematic representation of the macroscopic orientation anisotropy, S , that gives rise to the signal. When the field is on (excitation pulses are in the sample), the system evolves, developing a nonzero anisotropy. When the field goes off (pulses leave the sample), $S \neq 0$. S returns to zero by two processes: One is the structural relaxation that reforms the crooked T local structure, and the other is the rotational diffusion that finally returns S to zero.

(optical excitation pulses are in the sample), the potential minimum is shifted to a value with $S \neq 0$. The system evolves while the field is on. When the field is turned off (pulses have passed through the sample), the location of the potential minimum returns to $S = 0$. This leaves the sample with a macroscopic anisotropy, $S \neq 0$. This anisotropy decays through two distinct mechanisms. The fast relaxation (3.5 ps) labeled 1 is the structural relaxation that reforms the crooked T's. This removes part of the anisotropy. The remaining anisotropy decays by hydrodynamic rotational diffusion. This is labeled 2. The observation of the local structure relaxation as an exponential decay is quite reasonable, as relaxation on a parabolic potential surface has an exponential time dependence. The small perturbations due to the OKE interaction with the optical field are not likely to result in any deviations beyond the harmonic region of the intermolecular potential surfaces.

The dynamics of the local structure relaxation (τ_f) are temperature independent as long as the time scales for structure randomization, τ_i and τ_s , are long compared to τ_f . As the temperature is increased, the viscosity is reduced and τ_i and τ_s become faster. However, the viscosity is a property of the isotropic bulk liquid; it depends on the (relatively) long time scale behavior of the liquid. The local structure relaxation depends on the details of the local free energy surface, not on the bulk viscosity. As long as the local structures exist for a time great compared to τ_f , τ_f will be insensitive to the temperature dependence of the viscosity. (It is possible that τ_f has a weak temperature dependence,²⁰ e.g., $T^{1/2}$, that is not observed because of the limited range of temperatures over which the nonhydrodynamic behavior can be investigated.) When the temperature is raised sufficiently, τ_i and τ_s approach τ_f . At these elevated temperatures the local structures randomize on the τ_f time scale, and τ_f becomes temperature dependent.

The discussion up to this point has been concerned with the postlibrational dynamics. All of the data have been fit starting at approximately 4–5 ps after $t = 0$. The data at earlier times are dominated by librations and possibly CI effects. Collision-induced (also known as interaction-induced) effects are due to the breakdown of the approximation that the molecular polarizability of molecule i is unaffected by neighboring molecules. In reality, the dipole induced by the optical field on molecule i induces a dipole on molecule j . In the lowest order correction, these first-order dipole induced dipole (DID) terms are taken into account. Higher order corrections account for the effect of the DID upon other molecules. On average, the DID contributions

from neighboring molecules cancel each other out. On a sufficiently fast time scale, however, molecular translational motion breaks this symmetry, and an individual molecule experiences a nonzero net DID polarizability. Translational motions only need to break the symmetry of the surrounding "shell" and, contrary to the name, do not need to involve direct collisions *per se*.

Molecular dynamic simulations have been done on a number of molecules, including diatomic fluids^{35,36} and CS₂.³⁶⁻³⁸ The general conclusion of these investigators, which should be representative of most organic liquids, is that there is a separation of time scales between the rotational diffusion term and the CI and cross terms. Specifically, the nonorientational terms are important on a fast (subpicosecond) time scale, and slower times are dominated by orientational dynamics. There is no time scale separation between CI effect and librational dynamics, however. Because there is no method to include CI effects in the study of the ultrafast librational dynamics, the common approach in the field is to not consider them explicitly. This may be reasonable since the signal from the excitation of librations is strong, and in a number of systems, oscillations in the signals arising from underdamped librations are clearly observed.

There are a number of theories that attempt to explain rotational dynamics on all time scales using librations as the fundamental event in molecular reorientation.³⁹⁻⁴³ The ideas incorporated into these theories, i.e., damping and dephasing, have been incorporated into phenomenological models by a number of workers, especially the Nelson and Kenney-Wallace groups.^{3,4,6,44} The librations will be modeled as over damped oscillators^{11,45}

$$G_{\text{lib}}^{\text{ee}} = A_1(e^{-t/\tau_1} - e^{-t/\tau_r}) \quad (8)$$

where τ_1 is the decay time and τ_r is the rise time of the librational signal. The finite rise time is due to the inertial response of the molecules to the "kick" of the subpicosecond optical pulse.

The nature of the contribution of the rotational diffusion component to the decay in the orientational anisotropy needs to be taken into account at short times. In some of the work, the rotational diffusion component was simply added to the librational component in the impulse response function.⁹ This is unphysical. A noninstantaneous rise of the rotational diffusion component was proposed by the Kenney-Wallace group in their explanation of the ultrafast dynamics.⁴⁴ The rise time of rotational diffusion is almost certainly coupled to the librational decay rate. The optical pulse (through stimulated Raman scattering) impulsively forces the molecules to begin to oscillate in phase. This perturbs the equilibrium ensemble of librational states that exist in the liquid. These librations occur in the potential wells formed by the surrounding molecules. The solvent shells and thus the potential wells evolve around the partially aligned molecules as they continue to librate coherently. As the librations thermalize (damp and/or dephase), the molecules librate in their new potential wells with an equilibrium ensemble of amplitude and phase factors, and the librational component of the orientational anisotropy disappears. However, there exists some residual anisotropy due to the fact that the librations thermalized while the molecules were still partially aligned with the optical field. (If the end result of the thermalization were a completely isotropic system, there would be no remaining anisotropy.) It is this residual anisotropy that decays by orientational relaxation, which in 2EN is composed of the structural relaxation and rotational diffusion (processes 1 and 2 in Figure 8). The orientational relaxation component of the signal must grow in as the coherent motions of the librations thermalize. A simple model for this coupling was proposed by Deeg *et al.*¹¹ The rise of the orientational

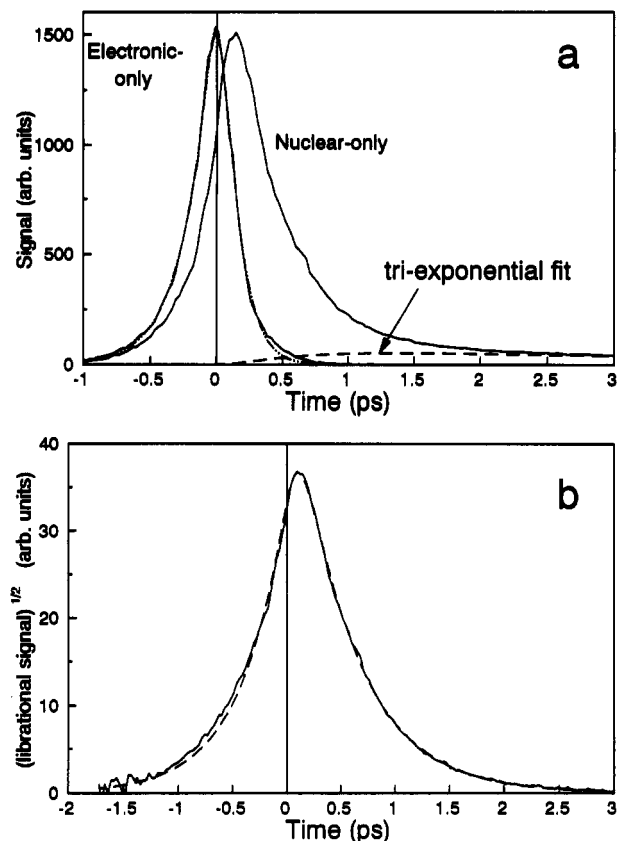


Figure 9. Ultrafast components to the decay of the orientational anisotropy for neat 2En at 2 °C. (a) Raw data and fits for the nuclear and electronic components of the OKE are graphed. The electronic-only data give the instrument response of the system. The fit to the electronic response with a double-sided exponential pulse shape is shown. The nuclear component is shown with the dashed curve giving the triexponential postlibrational contribution. Note the separation of the peak of the electronic and nuclear responses. (b) Librational only data with the dashed curve of a removed are presented along with the fit to the data.

relaxation is given by the decay of the librational contribution, i.e.,

$$G_{\text{OR}_i}^{\text{ee}} = \sum_i A_{\text{OR}_i} (1 - e^{-t/\tau_1}) e^{-t/\tau_{\text{OR}_i}} \quad (9)$$

where τ_1 is the decay time of the libration in eq 8 and τ_{OR_i} is the *i*th orientational relaxation time constant.

The librational data is taken with a polarization configuration that allows observation of the nuclear OKE without contamination from the electronic OKE.^{2,46} The polarizations of the first- (adjacent to the probe) and second-excitation beams, the probe, and the signal are 0, 45, 90°, and β , respectively. β is the orientation of a polarizer placed in the signal path. The value of β for nulling out the electronic response (i.e., observing the nuclear response) is 135°. The nuclear response is nulled out at $\beta = 56.3^\circ$. Figure 9a shows the nuclear-only OKE data for neat 2EN at 2 °C; a dashed curve represents the triple-exponential component of the data including the rise with $\tau_1 = 500$ fs (eq 9), and for comparison, the electronic-only OKE data. The electronic OKE data provide us with the instrument response of the system. One should note the very small amplitude of the orientational relaxation components relative to the peak.

The librational components are analyzed in the following manner. The square roots of the nuclear-OKE data are taken, and the triexponential fits for the orientational relaxation data (with the 500 fs build in) are subtracted out. As the remaining data need to be analyzed at delay times when the probe pulse is overlapping the excitation pulses, a convolution of the data with the pulse shape, obtained from the instrument response, is

necessary. The transient grating signal is of the form

$$S(t) = \int_{-\infty}^{+\infty} I_p(t''-t) \left[\int_{-\infty}^{t''} G^{ee}(t''-t') I_e(t') dt' \right]^2 dt'' \quad (10)$$

where I_p is the pulse shape of the probe pulse and I_e is the pulse shape of the excitation pulses, which are the same in these experiments. The pulse shape can be determined by fitting the electronic response to eq 10 using a δ -function impulse response function. The pulse can be very well modeled by a double-sided exponential model function, with $\tau_{\text{rise}} = 77$ fs and $\tau_{\text{fall}} = 207$ fs. As can be seen in the "electronic-only" trace of Figure 9a, the pulse shape fit is very good.

The fit to the nuclear OKE uses the square root of the convolution of eq 10, as the square roots of the data were taken to subtract out the orientational relaxation contributions. The librational data and the fit are shown in Figure 9b. The impulse response function used to generate the fit is the overdamped oscillator of eq 8. The inclusion of two librational terms is necessary to properly fit the data. The librational decay time constants are 52 ± 5 fs and 520 ± 20 fs, and the best fit for the librational rise time is 20 fs. Because the rise is very fast compared to the pulse duration, the error bars are quite large ($> \pm 50\%$). Because of the large amplitude of the librational component as compared to the orientational relaxation components, the exact form of the coupling of the librational decay and the rise of orientational relaxation components (eq 9) will have relatively little effect on the fit of the librational dynamics. The very good fit of the librational data adds confidence in the use of the triexponential model for the description of the postlibrational dynamics.

Concluding Remarks

We have monitored the orientational dynamics of neat 2EN for over 27 factors of e (12 decades) in signal decay, with the postlibrational orientational relaxation accounting for 22 factors of e (> 9 decades). The postlibrational dynamics are fit by a triple-exponential decay and display both hydrodynamic and nonhydrodynamic orientational dynamics. The slower two components of the decay correspond to rotational diffusion and behave hydrodynamically. A third component is attributed to the relaxation of the local liquid structure of 2EN, which is temperature independent from 2 to 40 °C. This demonstrates a decoupling of the local structure relaxation from the bulk viscosity. The dynamics of low-concentration 2EN solutions support this interpretation, as the solutions (which lack local structure) exhibit only biexponential decays which are hydrodynamic. The ultrafast librational dynamics have been fit with an overdamped oscillator model, revealing two distinct decay times and a finite inertial rise time for the librations.

Recently there has been considerable interest in liquid dynamics and the role it plays in time-dependent fluorescence spectral shifts^{47,48} and chemical reactions.⁴⁹ Hydrodynamic models work only moderately well in describing these dynamical processes in liquids. More detailed models, e.g., the mean spherical approximation,^{50,51} can provide somewhat better descriptions. However, the results presented here suggest that the details of anisotropic intermolecular interactions, which give rise to local structures, can have a dramatic influence on dynamical phenomena occurring in liquids. Local structures can exist on a time scale short compared to the rotational diffusion time. On this short time scale, dynamics can be controlled by an essentially fixed potential surface. An optical or thermal perturbation of the local structure results in relaxation back to the preferred structure, rather than diffusive randomization. This results in viscosity-independent and essentially temperature-independent dynamics. Changing the viscosity changes the time scale for the loss of the local

structure. However, so long as the local structure exists for a time long compared to the relaxation time of the perturbed local structure, dynamics will be controlled by the nature of the potential surface, not by viscosity-dependent hydrodynamic rotational diffusion.

Acknowledgment. This work was supported by the National Science Foundation, Division of Materials Research (Grant DMR90-22675).

References and Notes

- (1) Greene, B. I.; Farrow, R. C. *Chem. Phys. Lett.* **1983**, *98*, 273.
- (2) Etchepare, J.; Grillon, G.; Chambaret, J. P.; Hamoniaux, G.; Orszag, A. *Opt. Commun.* **1987**, *63*, 329.
- (3) Ruhman, S.; Kohler, B.; Joly, A. G.; Nelson, K. A. *Chem. Phys. Lett.* **1987**, *141*, 16.
- (4) McMorrow, D.; Lotshaw, W. T.; Kenney-Wallace, G. A. *IEEE J. Quantum Electron.* **1988**, *QE-24*, 443.
- (5) Hattori, T.; Kobayashi, T. *J. Chem. Phys.* **1991**, *94*, 3332.
- (6) Ruhman, S.; Nelson, K. A. *J. Chem. Phys.* **1991**, *94*, 859.
- (7) Lotshaw, W. T.; McMorrow, D.; Kalpouzos, C.; Kenney-Wallace, G. A. *Chem. Phys. Lett.* **1987**, *136*, 323.
- (8) Lotshaw, W. T.; McMorrow, D.; Kenney-Wallace, G. A. *Proc. SPIE* **1988**, *981*, 20.
- (9) Ruhman, S.; Kohler, B.; Joly, A. G.; Nelson, K. A. *IEEE J. Quantum Electron.* **1988**, *QE 24*, 470.
- (10) McMorrow, D.; Lotshaw, W. T. *Chem. Phys. Lett.* **1990**, *174*, 85.
- (11) Deeg, F. W.; Stankus, J. J.; Greenfield, S. R.; Newell, V. J.; Fayer, M. D. *J. Chem. Phys.* **1989**, *90*, 6893.
- (12) Deeg, F. W.; Greenfield, S. R.; Stankus, J. J.; Newell, V. J.; Fayer, M. D. *J. Chem. Phys.* **1990**, *93*, 3503.
- (13) de Gennes, P. G. *The Physics of Liquid Crystals*; Clarendon: Oxford, U.K., 1974.
- (14) Stankus, J. J.; Torre, R.; Fayer, M. D. *J. Phys. Chem.* **1993**, *97*, 9478.
- (15) (a) Sengupta, A.; Terazima, M.; Fayer, M. D. *J. Phys. Chem.* **1992**, *96*, 8619. (b) Sengupta, A.; Fayer, M. D. *J. Chem. Phys.*, accepted for publication.
- (16) Newell, V. J.; Deeg, F. W.; Greenfield, S. R.; Fayer, M. D. *J. Opt. Soc. Am. B* **1989**, *6*, 257.
- (17) von Jena, A.; Lessing, H. E. *Opt. Quantum Electron.* **1979**, *11*, 419.
- (18) Eyring, G.; Fayer, M. D. *J. Chem. Phys.* **1984**, *81*, 4314.
- (19) Favro, D. *Phys. Rev.* **1960**, *119*, 53.
- (20) Berne, B. J.; Pecora, R. *Dynamic Light Scattering*; Wiley: New York, 1976.
- (21) Yan, Y.; Nelson, K. A. *J. Chem. Phys.* **1987**, *87*, 6257.
- (22) Debye, P. *Polar Molecules*; Dover: New York, 1929.
- (23) Kivelson, D. In *Rotational Dynamics of Small and Macromolecules*; Dorfmueller, T., Pecora, R., Eds.; Springer: Berlin, 1987; p 1.
- (24) Perrin, F. *J. Phys. Radium.* **1934**, *5*, 497.
- (25) Hu, C.; Zwanzig, R. *J. Chem. Phys.* **1974**, *60*, 4354.
- (26) Youngren, G. K.; Acrivos, A. *J. Chem. Phys.* **1975**, *63*, 3846.
- (27) Alms, G. R.; Bauer, D. R.; Brauman, J. I.; Pecora, R. *J. Chem. Phys.* **1973**, *58*, 5570.
- (28) Keyes, T.; Kivelson, D. *J. Chem. Phys.* **1972**, *56*, 1057.
- (29) Kivelson, D.; Madden, P. A. *Annu. Rev. Phys. Chem.* **1980**, *31*, 523.
- (30) Alms, G. R.; Bauer, D. R.; Brauman, J. I.; Pecora, R. *J. Chem. Phys.* **1973**, *59*, 5310.
- (31) Ruessink, B. H.; MacLean, C. *Mol. Phys.* **1987**, *60*, 1059.
- (32) Hirschfelder, J. O.; Curtiss, C. F.; Bird, R. B. *Molecular Theory of Gases and Liquids*; Wiley: New York, 1954.
- (33) Misawa, M.; Fukunaga, T. *J. Chem. Phys.* **1990**, *93*, 3495.
- (34) McMorrow, D.; Lotshaw, W. T. *Chem. Phys. Lett.* **1993**, *201*, 369.
- (35) Frenkel, D.; McTague, J. P. *J. Chem. Phys.* **1980**, *72*, 2801.
- (36) Geiger, L. C.; Ladanyi, B. M. *J. Chem. Phys.* **1987**, *87*, 191.
- (37) Madden, P. A.; Tildesley, D. J. *Mol. Phys.* **1985**, *55*, 969.
- (38) Geiger, L. C.; Ladanyi, B. M. *Chem. Phys. Lett.* **1989**, *159*, 413.
- (39) Hill, N. E. *Proc. Phys. Soc.* **1963**, *82*, 723.
- (40) Lassier, B.; Brot, C. *Chem. Phys. Lett.* **1968**, *1*, 581.
- (41) Kushick, J. N. *J. Chem. Phys.* **1977**, *67*, 2068.
- (42) Lynden-Bell, R. M.; Steele, W. A. *J. Phys. Chem.* **1984**, *88*, 6514.
- (43) Deb, S. K. *Chem. Phys.* **1988**, *120*, 225.
- (44) Kalpouzos, C.; McMorrow, D.; Lotshaw, W. T.; Kenney-Wallace, G. A. *Chem. Phys. Lett.* **1988**, *150*, 138.
- (45) Ruhman, S.; Williams, L. R.; Joly, A. G.; Kohler, B.; Nelson, K. A. *J. Chem. Phys.* **1987**, *91*, 2237.
- (46) Deeg, F. W.; Fayer, M. D. *J. Chem. Phys.* **1989**, *91*, 2269.
- (47) Maroncelli, M.; Fleming, G. R. *J. Chem. Phys.* **1987**, *86*, 6221.
- (48) Simon, J. D. *Acc. Chem. Res.* **1988**, *21*, 128.
- (49) Barbara, P. F.; Jarzeba, W. *Adv. Photochem.* **1990**, *15*, 1.
- (50) Lebowitz, J. L.; Percus, J. K. *Phys. Rev.* **1966**, *144*, 251.
- (51) Rips, I.; Kalfter, J.; Jortner, J. *J. Chem. Phys.* **1988**, *88*, 3246.